Spin thermodynamics and methyl tunnelling

1992 J. Phys.: Condens. Matter 4 4165

(http://iopscience.iop.org/0953-8984/4/16/016)

J. Phys.: Condens. Matter 4 (1992) 4165–4171. Printed in the UK

Spin thermodynamics and methyl tunnelling

M J Barlow, S Clough, P A Debenham and A J Horsewill
Department of Physics, University of Nottingham, Nottingham NG7 2RD, UK

Received 21 November 1991, in final form 17 February 1992

Abstract. Experiments are reported in which the populations of nuclear Zeeman and methyl tunnelling levels are manipulated by driving selected transitions in a sequence. Saturation bottlenecks can be avoided and the intensity of spectral lines enhanced by driving two transitions alternately and repetitively. The results are explained in terms of a two-temperature model. The method allows transitions between tunnelling levels that do not change the magnetization to be observed.

The measurement of nuclear spin–lattice relaxation time is an established and powerful way of studying molecular motion in crystals, but it is limited in providing only a single parameter. In some cases the relaxation is non-exponential and two or more parameters may be determined, though their analysis requires a model of the motion. These limitations arise because the relaxation rate is an average of many transition probabilities. Methyl tunnelling spectroscopy offers the opportunity for a much more detailed study of molecular motion because the different transitions that normally contribute to relaxation are separated spectroscopically. In addition to the relaxation transitions the relative probabilities due to applied fields may be studied through relative intensities and saturation effects. Finally the possibility exists at low temperatures that the tunnelling spectrum can be modified by external fields through the creation of rotating wavepacket excitations. These objectives require the development of appropriate experimental techniques to determine systematically the elements in a relaxation matrix. The experiments that we describe demonstrate the feasibility of such studies. In the interests of simplicity they are interpreted in terms of only two dynamical parameters, namely the nuclear Zeeman and methyl tunnelling reciprocal temperatures. They establish a simple experimental and conceptual framework for later elaboration and, in particular, they show that transitions that are not obviously visible may be made accessible to study.

Hindered methyl groups at low temperature exhibit a tunnelling splitting $\hbar\omega_t$ of the ground librational state with rotational species A and E, the latter subdividing into E_a and E_b. The relative populations define a tunnelling temperature θ_t.

$$p(E)/p(A) = \exp(-\beta_t\omega_t) \tag{1}$$

where $\beta_t = \hbar/k\theta_t$. If the conversion time is long, θ_t may be very different from the lattice temperature. A number of level-crossing magnetic resonance techniques [1–4] for measuring the tunnel frequency ω_t depend on detecting the resonant transfer of energy between the tunnelling energy reservoir and a nuclear Zeeman reservoir whose

0953-8984/92/164165+07$04.50

reciprocal temperature $\theta_Z^{-1} = k\beta_Z/\hbar$ is proportional to the nuclear magnetization and easily monitored. In these cases the transfer mechanism involves internal interactions like the inter-nuclear dipole–dipole interactions rather than external fields. It is generally expected that externally applied fields cannot drive conversion transitions because they are uniform across the methyl triangle. We have found that for small tunnel frequencies of the order of a few hundred kHz this prohibition does not apply and θ_t may readily be changed by means of an applied oscillating magnetic field at the frequency ω_t. This enables the populations of the tunnelling and Zeeman energy levels to be manipulated in various ways to enhance the intensities of some spectral lines and to allow relative transition probabilities to be studied from the modified spectra. In this work we describe the new technique with some preliminary examples.

The basic experimental method is low-field magnetic resonance using field cycling [5]. It is carried out at 4.2 K where nuclear spin–lattice relaxation times are several minutes. By preparing a standard nuclear magnetization at high field, switching rapidly (2 s) to a low field for the experiment and returning to the high field for the measurement of the remaining magnetization, the advantages of high and low fields are combined. The sensitivity associated with high-field NMR is retained while the nuclear Zeeman, dipolar and methyl tunnel reservoirs are of comparable size during the experimental period at low field. At low field, transitions between A and E methyl species are allowed that are forbidden at high field [5]. During the period of about 10–30 s at low field, one or more oscillating fields may be applied to the sample simultaneously or sequentially, and their effect in changing the magnetization remaining after the sequence is measured. The preparation–experiment–measurement cycle is repeated many times while incrementing the frequency of one of the oscillating fields. The dependence of the residual magnetization on this frequency provides a magnetization destruction spectrum. A spectrum consists of a series of holes burned into a flat background, but for presentation we invert the spectrum and refer to peaks. The main peak occurs at the nuclear Larmor frequency, with one of lesser strength at twice this frequency. Each has a pair of sidebands separated from the parent peak by the methyl tunnel frequency ω_t. A seventh peak, normally very small, occurs at the tunnel frequency ω_t. The intensities of these peaks depend on the tunnel and nuclear Zeeman temperatures and the temperatures are modified by irradiation of the peaks. This allows the tunnelling temperature to be manipulated and a considerable enhancement of the peak ω_t to be achieved.

The peaks correspond to transitions between energy levels E_i identified by two numbers m_i, n_i, the magnetic and tunnelling quantum numbers:

$$E_i = \hbar\omega_Z m_i + \hbar\omega_t n_i. \tag{2}$$

The number n_i is defined to be 1/2 for E and $-1/2$ for A states, while m_i runs from 3/2 to $-3/2$ in integral steps for A and is $\pm 1/2$ for E_a and E_b. The E levels are doubly degenerate. The populations p_i of the levels are governed by β_t and β_Z. Ignoring constants since we are only interested in population differences and expanding the Boltzman factors we have

$$p_i = \beta_Z m_i \omega_Z + \beta_t n_i \omega_t. \tag{3}$$

Energy-conserving processes restore the simple relationship (3) when transitions change the populations of some of the levels [6]. The reciprocal-temperature pa-

rameters are given in terms of the populations by

$$\beta_Z = \sum_i p_i m_i \Big/ \left(\omega_Z \sum m_i^2\right) \tag{4}$$

$$\beta_t = \sum_i p_i n_i \Big/ \left(\omega_t \sum_i n_i^2\right). \tag{5}$$

If a transition defined by i, j is driven continuously, the populations change until $p_i - p_j = 0$. The transition is then saturated. We restrict attention to those transitions that involve species conversion, namely those for which $\Delta n = \pm 1$, while Δm may be 0, 1 or 2. The saturation conditions follow from (3)

$$\beta_Z/\beta_t = -\omega_t \, \Delta n/\omega_Z \, \Delta m. \tag{6}$$

A single transition Δn, Δm can change the temperatures until (6) is satisfied when change stops. This limits the change in β_Z, the observed parameter. If a second transition with a different value of Δn is now driven it carries the system towards a different saturation condition. Then the first transition may be driven again. Alternately driving two transitions is thus much more efficient in changing β_Z than driving either separately. This is the basis of the experiments to be described.

The evolution of the two temperatures is conveniently described by a point moving in the β_Z, β_t plane. The direction in which it moves is determined by $\mathrm{d}\beta_Z/\mathrm{d}\beta_t$ obtained from (4) and (5). For a single transition only $\mathrm{d}p_i = \mathrm{d}p_j$ is non-zero and

$$\mathrm{d}\beta_t/\mathrm{d}\beta_Z = C\omega_Z \, \Delta n/\omega_t \, \Delta m \tag{7}$$

where $C = \sum m_i^2 / \sum n_i^2$ which is 5. The path from the initial values $\beta_t(0)$, $\beta_Z(0)$ is

$$\beta_t - \beta_t(0) = C\omega_Z \, \Delta n(\beta_Z - \beta_Z(0))/\omega_t \, \Delta m \tag{8}$$

which intersects (6) at $\beta_t(s)$, $\beta_Z(s)$, the values at which change would stop. The evolution towards these values is

$$\beta_Z(t) - \beta_Z(s) = (\beta_Z(0) - \beta_Z(s)) \exp(-Wt_1) \tag{9}$$

where W is the transition probability and t_1 the duration of the irradiation. The path is a line inclined to the β_Z axis and the inclination is reversed if Δn is reversed. By switching between a pair of transitions, progression across the β_Z, β_t plane in the direction of the β_t axis occurs in the manner of a yacht tacking. Progress on each tack falls exponentially as the lines (6) are approached, so the maximum reduction in the observable parameter β_Z is obtained by staying away from these lines. The initial values of β_Z and β_t depend on the mode of preparation and on the field switch. Thermal relaxation is slow and, because the external field is small, its effect is a superimposed slow drift towards $\beta_Z = \beta_t = 0$.

Figure 1(*a*) shows two paths on the β_Z, β_t plane starting from the point A. The lines S_1 and S_{-1} are the saturation lines (6) for $\Delta n = 1$ and -1. Each of the two paths shown from A is obtained by alternately irradiating two transitions. In one case the transitions have the same value of Δn and in the other case they are of opposite

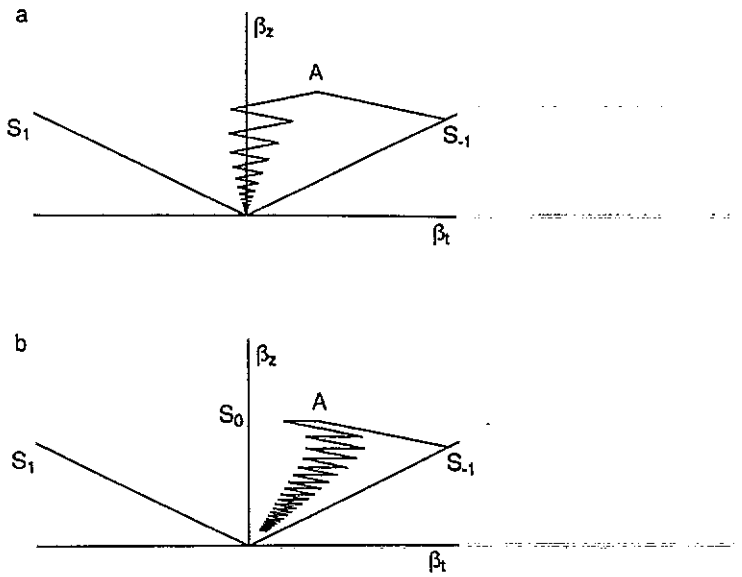

Figure 1. Diagrams showing the trajectory of the reciprocal-temperature parameters β_Z and β_t as two transitions are driven alternately. In (*a*) the two paths from A are for $\Delta n = \pm 1$ transitions, in one case with the same and in the other case with opposite signs. In (*b*) one of the paths is for alternating $\Delta m = 1$ and $\Delta m = 0$ transitions. The lines $S_{\Delta n}$ are saturation lines.

signs. In the first case the saturation effects are cooperative and the path stops on the S_{-1} line. The second zigzag path reduces β_Z, and hence the magnetization, very efficiently. Figure 1(*b*) is a similar diagram but now the second path switches between $\Delta m = 1$ and $\Delta m = 0$ transitions. The saturation line for the latter is $\beta_t = 0$. This transition is of special interest because it occurs at the tunnel frequency ω_t and because it does not itself cause any change in β_Z. It is apparent though that it has a considerable influence on the change in β_Z induced by the accompanying transition.

The experiments were carried out on methyl malonic acid whose methyl tunnel frequency is 75 ± 3 kHz [6]. The simplest experiment is to use a single oscillating field whose frequency is scanned to provide the spectrum. The lower trace in figure 2 shows the $\Delta m = 1$ transition and its $\Delta n = \pm 1$ satellites in this case. The data were obtained at a field of 6.5 mT. If the initial value of β_t were 0 the amplitudes of the two satellites would be equal since the starting points in the β_Z, β_t plane would be symmetrically disposed relative to the two saturation lines (6). A positive initial β_t makes the high-frequency satellite the more intense and this is universally found to be the case for the simple experiment. The upper trace in figure 2 shows the spectrum when two oscillating fields are applied alternately, each for 10 bursts of duration 0.5 s. One frequency is scanned as before and the second has the fixed frequency ω_t = 75 kHz. This experiment is represented by figure 2, upper part. The low-frequency satellite is enhanced and of similar, though not quite equal, intensity to its partner. This is achieved when $\gamma^2 B_1^2 g(\omega)\ \Delta t \sim 1$ where $\gamma^2 B_1^2 g(\omega)$ is the transition rate and Δt is the duration of the burst. Only relative values of B_1 are known. Figure 3 shows how the amplitude of the low-frequency $\Delta m = 1$ satellite depends on the second

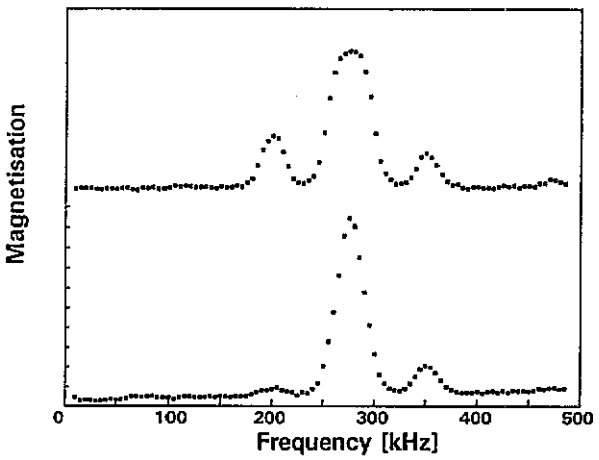

Figure 2. The $\Delta n = 1$ peak and its tunnelling satellites for methyl malonic acid. In the lower diagram only one frequency was used and in the upper diagram it alternated at 75 kHz. This corresponds to the zigzag trajectory of figure 1(*b*).

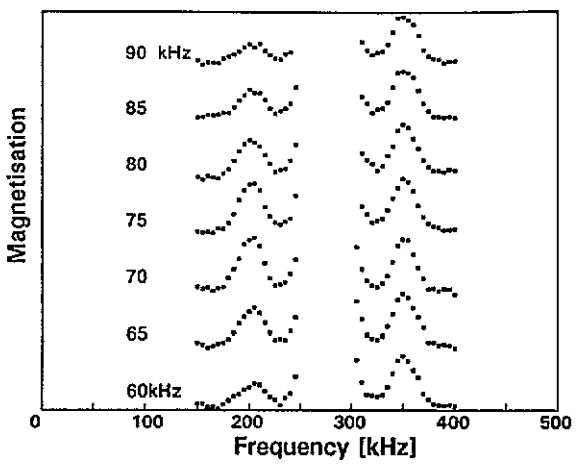

Figure 3. A set of spectra similar to the upper diagram of figure 2 but varying the second frequency from 60 to 90 kHz, and showing the resonant enhancement near 75 kHz.

frequency when the latter is varied between 60 and 90 kHz. This dependence traces a resonance curve similar in width to the satellite peaks themselves. The high-frequency satellite amplitude is only weakly dependent on the second frequency.

Figure 4 shows the effect when the second frequency is tuned to the satellites of the $\Delta m = 2$ peak. This enables the influence on the $\Delta m = 1$ satellites to be studied without direct interference from the second frequency. In this experiment the two frequencies alternated in 0.5 s bursts each for a total time of 10 s. The lower trace in figure 4 was obtained while irradiating the high-frequency $\Delta m = 2$, $\Delta n = 1$ satellite. The $\Delta m = 1$, $\Delta n = -1$ satellite is the stronger in the figure because the two driven transitions compensate each other's saturating effects. This is illustrated in figure 1(*a*). In the yachting analogy they are on opposite tacks. Conversely the

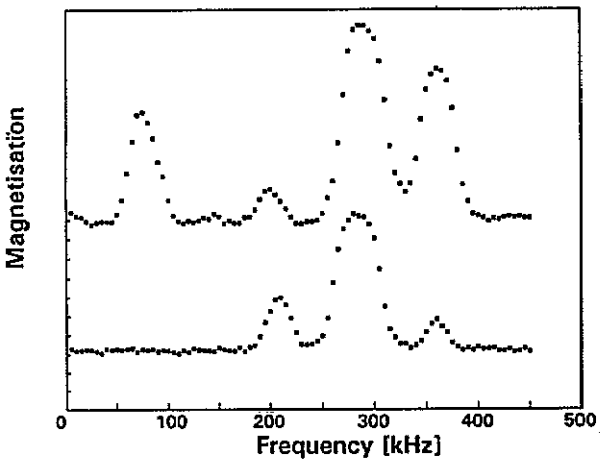

Figure 4. Spectra obtained when the second frequency is tuned to the $\Delta m = 2$, $\Delta n = +1$ (lower diagram) or $\Delta m = 2$, $\Delta n = -1$ (upper diagram) satellite. The peak at 75 kHz is missing in the lower diagram but appears in figure 5.

$\Delta m = 1$, $\Delta n = 1$ satellite is weakened by the extra saturation caused by the second oscillating field. The upper trace is obtained while irradiating the $\Delta m = 2$, $\Delta n = -1$ satellite and shows the opposite effect with enhancement of the $\Delta m = 1$, $\Delta n = 1$ satellite.

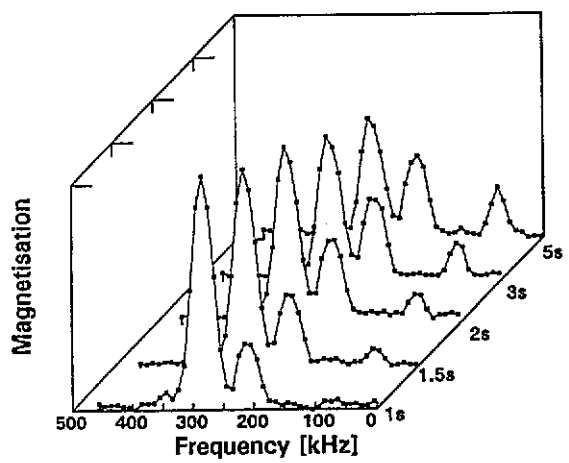

Figure 5. Data obtained as in the lower diagram of figure 4 but with the longer irradiation times shown on the figure, illustrating the progressive effect at 75 kHz.

The outstanding feature in the upper trace in figure 4 is the new peak at 75 kHz. The difference in its strength in the upper and lower diagrams is due to the fact that the starting value of β_t is positive. This makes the first burst of the second frequency more efficient at destroying the magnetization as can be seen from the smaller amplitude of the lower trace. Detailed simulations show that the effect at 75 kHz is less in this case and may even be negative. This initial effect diminishes in relative im-

portance when longer bursts are used. This is demonstrated in figure 5 which shows spectra like the lower diagram of figure 4 but with progressively increasing times.

The method makes possible a study of the relative transition probabilities and relaxation processes associated with individual transitions. It is potentially much more informative than either spin–lattice relaxation measurements or single-frequency spectroscopy. It may help to clarify the mechanism by which the conversion transitions are driven. In view of the uniformity of the oscillating fields across the dimensions of a methyl group and the selection rule arising from the C_3 symmetry, the transitions require the intervention of some local interaction. The appearance of strong $\Delta m = 2$ peaks leaves little doubt that the dipole–dipole interaction has a role in driving the transitions, and not merely in mixing the states between which transitions are driven, the explanation for the much weaker satellites observed at high field. The observation of the transitions has interesting implications. Changing populations means changing the diagonal elements of a density matrix. As the example of NMR shows, when diagonal elements are changed by a coherent oscillating field off-diagonal elements are also created. In CW NMR they are the consequence of forced nuclear precession and their components in phase and in quadrature with the component of the field rotating in the sense of the Larmor precession are the dispersion and the absorption signals. The analogue in methyl dynamics is forced tunnelling rotation. This occurs through a superposition of A and E states. When A and E_a wavefunctions are superposed the combination is a partially localized wavepacket rotating in a definite sense. A wavepacket formed by superposing A and E_b rotates in the opposite direction. The conversion transitions are thus accompanied by methyl rotation in the quantum domain. Ways of exploring this off-diagonal part of the methyl density matrix will be discussed in a later paper.

Acknowledgment

The authors are grateful for the support of the BP Venture Research Unit.

References

[1] Glattli H, Sentz A and Eisenkremer M 1972 *Phys. Rev. Lett.* **28** 871
[2] Clough S and Mulady B J 1973 *Phys. Rev. Lett.* **30** 161
[3] van Hecke P and Janssens G 1978 *Phys. Rev.* B **17** 2124
[4] Punkkinen M, Tuhoi J E and Ylinen E E 1976 *Chem. Phys. Lett.* **13** 265
[5] Clough S, Horsewill A J, McDonald P J and Zelaya F O 1985 *Phys. Rev. Lett.* **55** 1794
[6] Goldman M 1970 *Spin Temperature and Nuclear Magnetic Resonance in Solids* (Oxford: Clarendon) p 19
[7] Clough S and McDonald P J 1982 *J. Phys. C: Solid State Phys.* **15** L1039